Electrophysical properties of polycrystalline diamond films deposited from an abnormal glow discharge

A V Gaydaychuk, A V Kabyshev, F V Konusov, S A Linnik and G E Remnev
National Research Tomsk Polytechnic University, 30, Lenin Avenue, 634050, Tomsk, Russia

E-mail: konusov@hvd.tpu.ru

Abstract. Electrophysical properties of polycrystalline diamond films (PDF), deposited from the abnormal glow discharge, were obtained. The energetic and kinetic characteristics of surface dark and photoconductivity of PDF and their temperature, field and spectral dependences were investigated. Dominant carrier transport mechanisms, their type and the energetic spectrum of localized defect states were established. Current–voltage characteristics, photosensitivity and activation energy are determined by conductivity of PDF, which varies from 10^{-14} to 10^{-4} S depending on deposition conditions. Vacuum annealing of films up to 600–800 K stabilizes the electrical characteristics. Thermal stability of PDF properties higher than semiconductor films, deposited under nonequilibrium conditions by pulsed laser and ion ablation. PDF films not inferior on properties to films, obtained by alternative CVD methods. Electrical characteristics, mechanism of charge transport of PDF were caused by defects of different nature, the energetic levels of which are continuously distributed on energy in the band gap. Dominant n–type of activation conduction is complemented by hopping mechanism through the localized states distributed near the Fermi level with density $5.6\cdot10^{17}$–$2.1\cdot10^{21}$ eV^{-1} cm^{-3}. Trapping and recombination centers are heterogeneously distributed on grain boundaries.

1. Introduction

Unique chemical, mechanical, electrical and thermal, optical and photoelectrical properties of diamond contribute to its wide application in high–frequency, high–temperature electronics and semiconductor manufacturing of a special purpose [1–5]. Due to the limited possibility of using diamond single crystals and epitaxial diamond films, because of their high cost in the most appropriate instruments are the polycrystalline diamond films (PDF), which are obtained by developed methods of the chemical vapor deposition (CVD) [1–9]. PDF are successfully used for the production of stable radiation-resistant detectors of UV and ionizing radiation, as well as for laser and photodiode structures [1, 3]. Dielectric PDF are used for these purposes with conduction $\sigma=10^{-15}$–10^{-11} $S\cdot cm^{-1}$. Depending on the characteristics of polycrystalline structure of PDF, the content of alloying impurity atoms and defects of crystal structure, electrical characteristics, as well as the mechanism of the transport and type of the charge carriers vary widely in range $\sigma=10^{-6}$–10^{3} $S\cdot cm^{-1}$ [1, 3–15]. Investigations of peculiarities of the PDF electrical properties and reasons determining property changes and deposition conditions effect on characteristics are very important. Among the various PDF deposition methods, there are microwave plasma, hot filament, arc–jet and glow discharge CVD to be marked out. But each of them has a number of disadvantages: has a high cost and limited maximal deposition area; the growth rate is low and constant replacement of filaments is necessary, the disadvantages of arc–jet CVD method are

small deposition area and high gas consumption. Among the others, glow discharge CVD is considered to be an effective diamond film deposition method because of its simplicity and high growth rate.

The aims of the work are to determine the electrical and photoelectrical characteristics and dominant transport charge mechanism also, to examine the energetic spectrum and nature of localized defect levels in PDF films, deposited from plasma abnormal glow discharge.

2. Experimental

Methods of films deposition from abnormal glow discharge and the study of their structural features are described in detail in [2, 3]. We submit a new discharge system for diamond film deposition at AC abnormal glow discharge. In this process the discharge in form of a plasma line operates between two small electrodes, and the inter electrode spacing reaches 20 cm. The electrodes are moved away from the substrate and do not contaminate the film [2]. Dark surface conductivity σ and photoconductivity $\Delta\sigma_{ph}=\sigma_{ph}-\sigma$ (σ_{ph} is conductivity at lighting), photosensitivity $K(U, T, h\nu)=\Delta\sigma_{ph}/\sigma$ were measured at a constant voltage between the electrodes U=0.01–300 V, at temperature T=300–700 K and photon energy hν=1.5–4.0 eV. The electrodes were deposited on the surface by rubbing the soft graphite. Temperature dependences of the σ, $\Delta\sigma_{ph}(T)$ were approximated by equation for the activation mechanism

$$\sigma_a(T) = \sigma_0 \times e^{(-\varepsilon_\sigma / k \cdot T)}, \qquad (1)$$

where σ_0 – pre–exponential factor, ε_σ – activation energy, k – Boltzmann constant and equation for the hopping mechanism of transport between the localized states (LS) near the Fermi level E_F in frame model of Mott

$$\sigma_p(T) = \sigma'_0 \times e^{(-(T_0/T)^{0.25})}, \qquad (2)$$

where σ'_0 – pre-exponential factor, T_0–activation energy [16–18]. The density of states $N(E_F)$ was calculated from values T_0 according to [16–18]. The sign of the dominant charge carriers was determined from amplitude of the photo–stimulated currents I_{PhTSC} (T, hν, U=0) [16].

3. Result and discussion

Current voltage characteristic (CVC) I(U), field dependence of K(U) and characteristics of carrier transport ε_σ, σ_0, T_0, σ'_0, $N(E_F)$, I_{PhTSC} vary in thickness and deposition plane, due to the inhomogeneity of PDF properties (table 1). Quantitative differences in the parameters σ and $\Delta\sigma_{ph}$ were recorded from the growth smooth and opposite rough sides (figure 1). Conductivity from the growth side (samples 12, 42, 62) is higher than from the side of the substrate (samples 11, 31, 41, 51) and the ratio between K is opposite (table 1, figure 1). In vacuum σ in 1.1–1.3 times lower than in the air, due to the weak influence of the absorption currents. Only physical adsorption of molecules of atmospheric gases on the surface of PDF affects the change of σ(T). So, stable chemical bindings are not formed. CVC coincidence at U>0 and U<0 indicates a weak influence of volume space charge on σ and $\Delta\sigma_{ph}$. The annealing of the films before T_{ann}<600 K stabilizes the properties. CVC of the PDF, which having

Table 1. Electrical and photoelectrical characteristics of deposited PDF.

Sample number	σ (S)	ε_σ (eV)	$N(E_F)$ ($eV^{-1}\cdot cm^{-3}$)	R (nm)	E_g (eV)	$\alpha\cdot10^4$ (cm^{-1})	I_{PhTSC} (A)
11	$6\cdot10^{-11}$	0.21	$5.6\cdot10^{17}$	8.1	1.48	4.8	$-4\cdot10^{-11}$
12	$1.1\cdot10^{-4}$	0.007	$1.5\cdot10^{21}$	1.1	1.11	2.6	$-1\cdot10^{-8}$
31	$4\cdot10^{-10}$	0.12	$1.5\cdot10^{18}$	6.4	1.28	3.3	$-1\cdot10^{-11}$
41	$7\cdot10^{-10}$	0.15	$5.6\cdot10^{17}$	8.1	1.28	3.2	$-6\cdot10^{-11}$
42	$4\cdot10^{-9}$	0.08	$4.2\cdot10^{18}$	4.9	1.55	2.7	
51	$2\cdot10^{-13}$	0.09	$5\cdot10^{18}$	4.7		3.0	$-2\cdot10^{-13}$
62	$8\cdot10^{-13}$	0.12	$1.6\cdot10^{18}$	6.2		2.8	$-5\cdot10^{-13}$

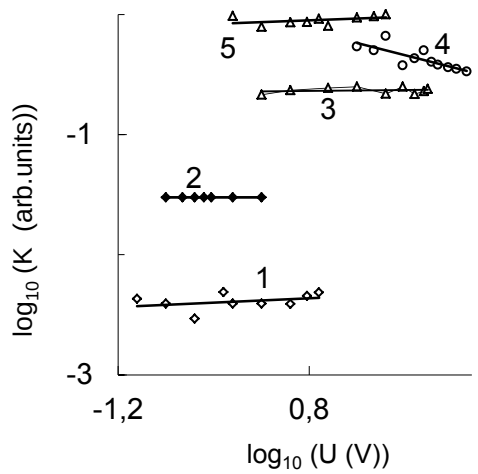

Figure 1. Field dependence of photosensitivity K(U) of PDF from the growth side (curves 1 and 2) and from the substrate side (curves 3–5) in the centre (curves 1,3) and on edge deposition (curves 2,4 and 5).

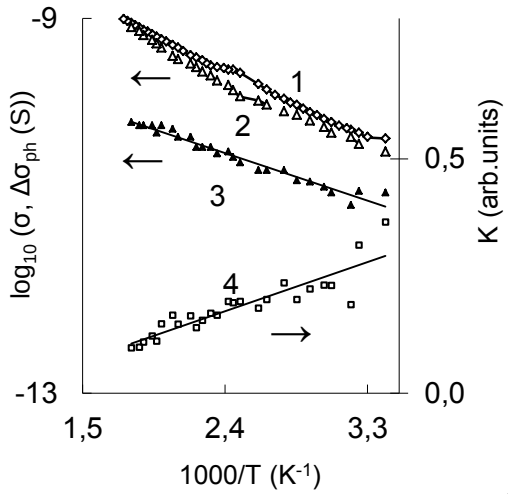

Figure 2. Temperature dependences of conductivity σ at the sequential heating (curves 1 and 2), photoconductivity $\Delta\sigma_{ph}$ (curve 3) and photosensitivity K (curve 4) of PDF from the growth side in the centre of deposition.

$\sigma=10^{-10}$–10^{-4} S is ohmic. These films have a low (K=0.005–0.1), but stable photosensitivity to heat and change U, as compared with dielectric PDF with K=0.1–1.0 (figure 1). In PDF with $\sigma=10^{-14}$–10^{-11} S deviation from the linear law is fixed and CVC obeys the equation $I\infty\exp(\beta U)$ (β=0.02–0.05) which indicates the effect from currents, limited by volume space charge, as in [8]. In CVC nonlinearity makes the spatial distribution of the energy barrier that exists on the border with electrodes and grain boundaries [6–8]. Variation in PDF electrical parameters may be caused by inhomogeneity in the distribution of crystallites on size and growth defects in their crystallites and on the boundaries or by the influence of hydrogen impurity in the surface layers [4, 11–14].

Dependences σ, $\Delta\sigma_{ph}(T)$ in interval T=300–600 K are determined by thermally stimulated electron exchange between the shallow donor levels with energy ε_σ=0.007–0.21 eV and the conduction band (CB) (figure 2). N–type σ and $\Delta\sigma_{ph}$ are dominated in PDF layers as shown I_{PhTSC} (T, hν) (table 1). At illumination the value ε_σ is lower at 0.03–0.05 eV than for σ by reducing the population of LS upon excitation by 5–10 times. There is usual thermal quenching of $\Delta\sigma_{ph}(T)$ at T≥340 K (figure 2, curve 4). It cannot be excluded the influence on characteristics the exchange of holes between LS defects and the valence band (VB) [13]. Differences in deposition methods reflect on the specific character of dependence $\sigma(\varepsilon_\sigma)$ of PDF films deposited from the abnormal glow discharge (figure 3). The electrical parameters indicate the effect on transport from the hopping conductivity, which is confirmed by approximation σ(T) by equation (2) in interval ΔT=300–600 K. Density of LS calculated from σ, $\Delta\sigma_{ph}(T)$ is $N(E_F)=5.6\cdot10^{17}$–$1.5\cdot10^{21}$ $eV^{-1}cm^{-3}$ in PDF with ε_σ=0.007–0.15 eV (table 1). In other PDF films a density of LS, exponentially distributed near E_F, consist $N(E_F)=(4–8)\cdot10^{19}$ [17, 18] and 10^{15}–10^{18} $eV^{-1}cm^{-3}$ [19]. The magnitude of the most probable jump length is calculated as in [16–18] for values $N(E_F)$ is R=1.1–8.1 nm and under lighting is reduced to 1.0–6.0 nm accordingly with the increase of the LS density in 3–5 times for PDF with $\sigma<10^{-10}$ S.

Dependences between the electrical parameters allow establishing the predominance of one transport charge mechanisms. Interrelation between σ, σ_0 and ε_σ indicates the predominance of activation transport (table 1, figure 3). This confirmed by interrelation $N(E_F)(\varepsilon_\sigma)$ which is typical for

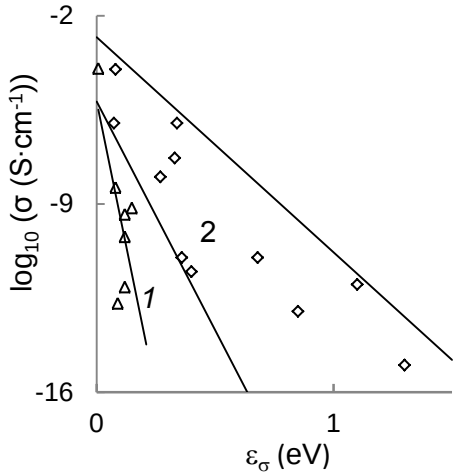

Figure 3. Interrelation between conductivity σ and activation energy ε_σ in PDF on our data (curve 1) and on literature data [4–7, 11] (curve 2).

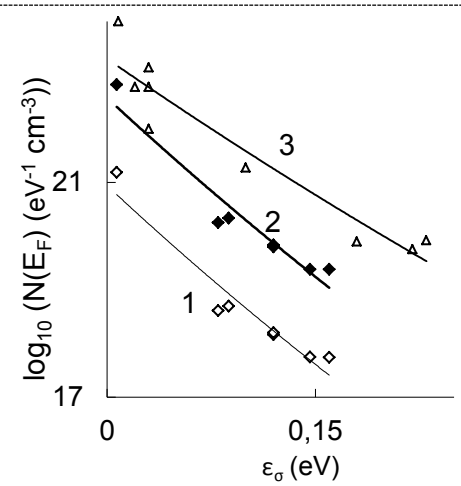

Figure 4. Interrelation between N(E_F) and ε_σ in PDF on our data (curves 1 and 2) and on literature data [17] (curve 3). Decay constant $\alpha=5.7\cdot10^6$ (curve 1) and $2\cdot10^7$ cm^{-1} (curve 2).

the uncrystalline semiconductors having a high content of defects (figure 4) [16–19]. By analogy with [6–13, 16–19], we can conclude that PDF hopping conductivity on LS near the Fermi level dominates over the activation in interval T=300–400 K. At T=400–600 K the characteristics of PDF is determined by the electrical conductivity activation $\sigma_a(T)$ with LS defects distributed on grain boundaries and localized in band gap (BG) in area of "tails" of the allowed bands. Charge carriers are excited through the mobility gap in the area of delocalized states. The relationship between the parameters σ'_0 and $T_0^{0.25}$, obtained in accordance with the equation (2), confirms the applicability of hopping transport through LS distributed near E_F, and demonstrates the differences in the structural

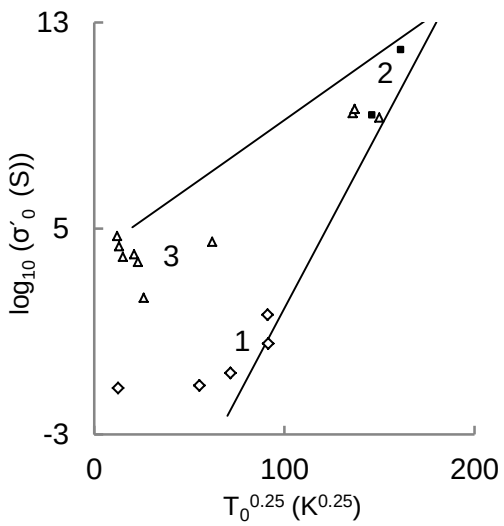

Figure 5. Interrelation between pre-exponential factor σ'_0 and activation energy $T_0^{0.25}$ (equation (2)) in PDF on our data (curve 1) and literature data [18] (points 2) and [17] (points 3).

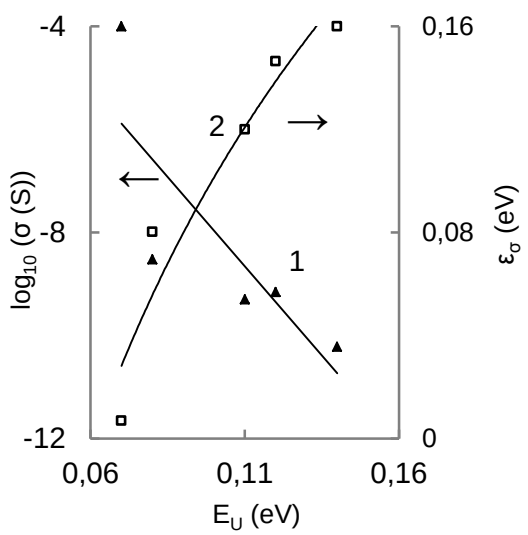

Figure 6. Interrelation between conductivity σ and Urbach energy E_U (curve 1) and activation energy ε_σ and E_U (curve 2) in PDF. Values E_U were calculated in the energetic interval hν=1.15–1.32 eV.

disorder (figure 5) [17, 18]. At T>600 K, the influence of the barrier between the crystallites is increases [6, 8]. The largest contribution to $\Delta\sigma_{ph}$ gives the activation component, as confirmed by K(T, U) (figures 1 and 2). The relationships between σ, ε_σ and direct BG width E_g, extracted from absorption spectra α(hν) in interval hν=1.5–4.2 eV, are consistent with the concept of carrier transport in amorphous or highly defective materials by exchange of carriers between CB and LS in its "tails" through the mobility gap (table 1) [1, 16]. Spectrum K(hν) is similar to α(hν) of PDF [1, 4]. A same spectra is proper to other PDF in intervals hν=1.8–2.9 eV and is typical for most structures in detectors of UV irradiation [4]. In work [12] a spectrum K(hν) was determined by electronic transitions between the VB and LS defects in thin oxidized layer after hydrogenation. Such a spectrum in nano–crystalline films was induced by transitions in LS of "tails" and levels belonging to graphite–like phases [1]. At that, oxygen arriving from the air and adsorbing on structural defects may have a passivation effect on the surface photosensitivity.

Accumulation of concentration of the optical active levels was connected with decreasing of LS density near the Fermi level which are participated in hopping transport, as it is shown by its reduction from $N(E_F)=10^{19}$ to $5\cdot10^{17}$ $eV^{-1}\cdot cm^{-3}$ an increase of the absorption coefficient from $\alpha=2\cdot10^4$ to $5\cdot10^4$ cm^{-1} (table 1). Reduction of conduction and LS density responsible for hopping transport are correlated also with an increase in ε_σ and in Urbach energy E_U of the optical active levels which determine α(hν) in intervals hν=1.15–1.3 eV and 1.6–3.0 eV (table 1, figure 6). Growth of its value from E_U=0.07 to 0.15 eV with the decreasing of conductivity from $\sigma=10^{-4}$ to 10^{-11} S and the increasing of the activation energy from ε_σ=0.007 to 0.16 eV is determined by influence on properties from the disorder induced with defects in the crystalline phase material due to the presence of disordered graphite–like phases in films. As a result, the exponential distribution of LS on energy is formed in BG of material [8, 17, 19].

4. Conclusion

Films deposited by abnormal glow discharge not inferior to films obtained by alternative CVD methods. Vacuum annealing of films up to 600–800 K stabilizes the electrical characteristics. Electrical and photoelectric characteristics, mechanism of transport charge in the deposited PDF are caused by the defects, the levels of which are continuously distributed on energy in the BG. Trapping and recombination centers of carriers are heterogeneously distributed in grain boundaries. Activation component of dark and photoconductivity of n–type is realized by exchange of the charge carriers between the conduction band and shallow donor levels with activation energy ε≤0.21 eV. Thermal quenching of photoconductivity is appeared. Activation conductivity was complemented by a hopping mechanism, involving localized states distributed in materials band gap near a Fermi level. Density of states, where the hopping conduction occurs, is significant $N(E_F)=5.6\cdot10^{17}$–$2.1\cdot10^{21}$ eV^{-1} cm^{-3}. Their variation over the surface and the film thickness is determined by content of the growth defects, heterogeneously distributed in the grain boundaries. Electrical and spectral parameters are subjected by strong effects from disorder induced by defects in crystallites and presence of disordered graphite–like phase in films.

Acknowledgments

The paper has been completed within megaproject of National Research Tomsk Polytechnic University «Materials for Extreme Conditions».

References

[1] Williams O A 2011 *Diamond and Relat. Mater*. **20** 621
[2] Linnik S A and Gaydaychuk A V 2013 *Diamond and Relat. Mater*. **32** 43
[3] Linnik S A and Gaydaychuk A V 2012 *Tech. Phys. Lett.* **38** 258
[4] Polyakov V I, Rukovishnikov A I, Avdeeva L A, Kun'kova Z E, Varnin V P, Teremetskaya I G and Ralchenko V G 2006 *Diamond and Relat. Mater.* **15** 1972
[5] Chiquito A J, Berengue O M, Diagonel E, Galzerani J C 2007 *J. Appl. Phys.* **101** 033714

[6] Kopylov P G, Lotonov A M, Apolonsky I A and Obraztzov A N 2009 *Vestn. of MSU. ser. 3(In Russian)* 2 54
[7] Trucchi D M, Cappelli E, Conte G, Mattei G, Gramaccioni C and Ascarelli P 2005 *Diamond and Relat. Mater*. **14** 575
[8] Conte G, Rossi MC, Spaziani F and Arcangeli R 2005 *Diamond and Relat. Mater.* **14** 570
[9] Hikavyy A, Clauws P, Maes J, Moshchalkov V V, Butler J E, Feygelson T, Williams O A, Daenen M and Haenen K 2006 *Phys. status solidi* **A 203** 3021
[10] Muret P and Saby Ch 2004 *Semicond. Sci. and Technol.* **19**1
[11] Hubik P, Mares J J, Kozak H and Kromka A 2012 *Diamond and Relat. Mater.* **34** 63
[12] Stallhofer M, Seifert M, Hauf M V, Abstreiter G, Stutzmann M, Garrido J A and Holleitner A W 2010 *Appl. Phys. Lett.* **97** 111107
[13] Yutaka Itoh, Yu Sumikawa, Hitoshi Umezawa and Hiroshi Kawarada 2006 *Appl. Phys. Lett.* **89** 203503
[14] Chaudhary A, Welch J O and Jackman R B 2010 *Appl. Phys. Lett.* **96** 242903
[15] Ri Sung-Gi, Takeuchi Daisuke, Kato Hiromitsu, Ogura Masahiko, Makino Toshiharu, Yamasaki Satoshi, Okushi H, Rezek B and Nebel Ch E 2005 *Appl. Phys. Lett.* **87** 262107
[16] Kabyshev A V, Konusov F V, Remnev G E and Pavlov S K 2013 *Proc. of the universities. Physics (In Russian)* **56** 30
[17] Achatz P, Williams O A, Bruno P, Gruen D M, Garrido A and Stutzmann M 2006 *Phys. Rev.* **B 74** 155429
[18] Gan L, Bolker A, Saguy C, Kalish R, Tan D L, Tay B K, Gruen D and Bruno P 2009 *Diamond and Relat. Mater.* **18** 1118
[19] Nath S and Wilson J I B 1996 *Diamond and Relat. Mater.* **5** 65